

On the birefringence of magnetoelectric BiFeO₃

RIVERA, Jean-Pierre, SCHMID, Hans

Abstract

The birefringence dispersion of a ferroelastic single domain of magnetoelec. BiFeO₃ crystal was measured at room temp. (24°) in the rhombohedral phase. A thin (11 μm) (110)cubic cut was used although it was not a principal cut. The optical axis (and spontaneous polarization) formed an angle of 35° with the normal to the cut. Due to anomalous interference colors, the right order was deduced with the help of conoscopy. The birefringence of this cut shows normal dispersion and its value is very large (dn' = 0.13 at λ = 550 nm to 0.08 at λ = 850 nm). The principal birefringence (dn = 0.34 at λ = 550 nm) was evaluated with the help of the computed (Gladstone-Dale relationship) mean refractive index ($n_m = 2.62$). From dn'(T), (8K < T < 820 K) the Neel temp. was found for the 1st time optically, TN = 653 K (380°), and a crit. exponent was tentatively derived near TN.

Reference

RIVERA, Jean-Pierre, SCHMID, Hans. On the birefringence of magnetoelectric BiFeO₃. *Ferroelectrics*, 1997, vol. 204, no. 1, p. 23-33

DOI : 10.1080/00150199708222185

Available at:

<http://archive-ouverte.unige.ch/unige:31139>

Disclaimer: layout of this document may differ from the published version.



UNIVERSITÉ
DE GENÈVE

ON THE BIREFRINGENCE OF MAGNETOELECTRIC BiFeO₃

J.-P. RIVERA and H. SCHMID

*Department of Mineral, Analytical and Applied Chemistry,
University of Geneva, Sciences II, 30 quai Ernest-Ansermet, CH-1211
Geneva 4, Switzerland*

(Received in final form 15 May 1997)

The birefringence dispersion of a ferroelastic single domain of magnetoelectric BiFeO₃ crystal has been measured at room temperature (24°C) in the rhombohedral phase. A thin (11 µm) (110)_{cubic} cut was used although it was not a principal cut. The optical axis (and spontaneous polarization) formed an angle of 35° with the normal to the cut. Due to anomalous interference colors, the right order was deduced with the help of conoscopy. The birefringence of this cut shows normal dispersion and its value is very large ($dn' = 0.13$ at $\lambda = 550$ nm to 0.08 at $\lambda = 850$ nm). The principal birefringence ($dn = 0.34$ at $\lambda = 550$ nm) has been evaluated with the help of the computed (Gladstone-Dale relationship) mean refractive index ($\bar{n} = 2.62$).

From $dn'(T)$, ($8 \text{ K} < T < 820 \text{ K}$) the Néel temperature has been found for the first time optically, $T_N = 653 \text{ K}$ (380°C), and a critical exponent has tentatively been derived near T_N .

Keywords: BiFeO₃; bismuth ferrite; dispersion of birefringence; birefringence vs. temperature; Néel temperature; antiferromagnetic phase transition; linear magnetoelectric effect; photoelastic modulator

INTRODUCTION

The perovskite BiFeO₃ has attracted much attention for many years because this material is known to have two types of long range order: simultaneous antiferromagnetic and ferroelectric ordering^[1, 2]. The known sequence of phase transitions is the following^[3, 4]:

Cubic ($Pm\bar{3}m1'$) \Rightarrow 1195 K \Leftarrow orthorhombic \Rightarrow 1100 K \Leftarrow rhombohedral ($R3c1'$) \Rightarrow $T_N \approx 653 \text{ K}$ (380°C) \Leftarrow average rhombohedral/antiferromagnetic/incommensurate, at least down to 4.2 K. The rhombohedral phase is ferroelectric/ferroelastic. This structure becomes antiferromagnetic below

T_N , with a unusual magnetic long range modulation and a cycloidal spiral length of 620\AA ^[1]. At $T=294\text{ K}$ ^[5] $a_{\text{hex}}=5.57874(16)\text{ \AA}$, $c_{\text{hex}}=13.8688(3)\text{ \AA}$, $Z_{\text{hex}}=6$, $a_{\text{rh}}=5.6343\text{ \AA}$, $\alpha_{\text{rh}}=59.348^\circ$, $Z_{\text{rh}}=2$ and $D_x=8.337\text{ g/cm}^3$. Only the bilinear magnetoelectric (ME_H) effect ($P_i=\beta_{ijk}H_jH_k$, i.e., a small electrical polarization induced by a magnetic field) has been measured at low magnetic field and at 4.2 K ^[6] (thus much below T_N), but not the linear one, which would be allowed in Shubnikov point group $3m$. All four allowed coefficients β_{111} , β_{113} , β_{311} and β_{333} were determined (axis $3//\vec{P}_s$, the spontaneous polarization). Note that axis y (axis 2), instead of axis x (axis 1), was chosen to be perpendicular to a mirror plane, thus β_{111} was given instead of β_{222} ! The linear ME_H effect ($P_i=\alpha_{ij}H_j$) was not observable, apparently because of canceling due to the cycloidal spiral structure. A magnetically induced phase transition has been found at strong magnetic field (200 kOe) and temperatures between 10 K and 150 K, with a large change of electrical polarization^[7,8]. Figure 2, curve z, of ref.^[7] (or (Fig. 1a), curve 3, of ref.^[8]), shows the induced polarization vs. magnetic field, \vec{P} and \vec{H} being along a pseudocubic $\langle 001 \rangle_{\text{cub}}$ direction ($\langle 001 \rangle_{\text{cub}}$). It allows us to estimate a coefficient of the linear ME effect in the high magnetic field induced phase, i.e., α (18 K) $\approx 0.52\text{ ps/m}$ or $1.6 \cdot 10^{-4}$ in Gaussian unit. This is a weak value, but probably a lower limit, since the pulsed magnetic field ME

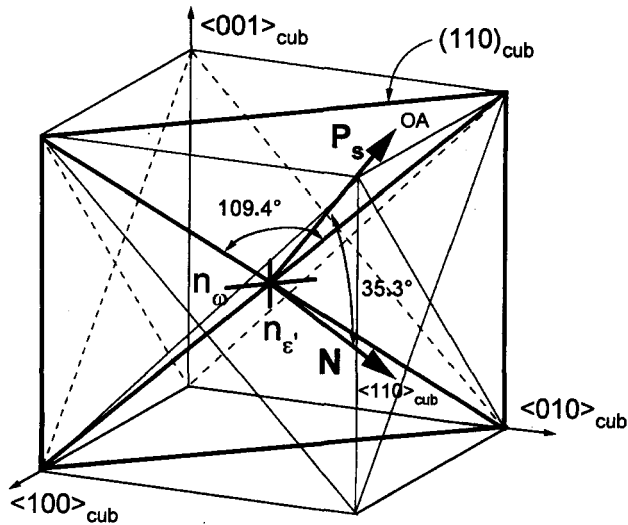


FIGURE 1 Schematic view of a $(110)_{\text{cub}}$ cut BiFeO_3 thin crystal (above T_N , point group $3m1'$), with the spontaneous polarization \vec{P}_s (parallel to the optical axis OA) inclined at 35.3° to the normal of the cut (\vec{N}). The axes (n_o, n_e) of the section of the optical are also shown. For convenience, superposed at the center of the crystal, traces of $(011)_{\text{cub}}$ and $(101)_{\text{cub}}$ thin walls.

measurements were done on unpoled ferroelectric/ferroelastic polydomain crystals.

With a view to future well defined high magnetic field ME measurements on ferroelectric/ferroelastic single domains, an improved knowledge of the spontaneous linear birefringence is mandatory for sample preparation. Earlier birefringence experiments^[3] at room temperature, on bismuth ferrite (BiFeO₃) showed a very high value, close to $dn = 0.6$ on a principal cut (a (110)_{cub} cut) and a strange birefringence dispersion curve ($dn'(\lambda)$) on another (110)_{cub} cut, with a minimum at 600 nm. Some doubts subsisted concerning the right compensation order found with tilting compensators. The dark compensation line observed at 8 K was not consistent with the one at 293 K, when the temperature was varied continuously. Hence a reappraisal becomes necessary. As the refractive indices are not known, a mean refractive index has been computed^[9] using the Gladstone-Dale relationship^[10]: $\bar{n} = 2.62$. These crystals are uniaxial optically negative, i.e., $\omega > \varepsilon' > \varepsilon$ (this has been reconfirmed), where ω and ε are the ordinary and extraordinary refractive indices, respectively.

The aim of the present work was to find at room temperature, the dispersion of the birefringence $dn' = \omega - \varepsilon'$ vs. wavelength, of a (110)_{cub} cut and then try to deduce the principle birefringence ($dn (= \omega - \varepsilon)$ vs. λ). Unfortunately, no sufficiently thin and sufficiently large single domain principal cuts were obtained, so as to measure dn directly. The temperature dependence of dn' was measured in order to obtain T_N because in the literature a large discrepancy exists between reported values, see e.g.,^[9] ranging between 300°C and 400°C. To our knowledge, T_N was never detected optically.

EXPERIMENTAL

Dendritic single crystals of BiFeO₃ were obtained by a Bi₂O₃/Fe₂O₃ flux growth method^[9]. This method gives (110)_{cub} leaflets from which thin (110)_{cub} platelets were prepared. The size of these crystals was about 1 to 3 mm, but the useful working diameter was about 100 μm or less. Most of the optical experiments presented here were performed on a platelet with thickness $t \approx 11 \mu\text{m}$ ($\pm 1 \mu\text{m}$).

The (110)_{cub} cuts present usually traces of inclined walls due to (011)_{cub}, (0 $\bar{1}\bar{1}$)_{cub}, (101)_{cub} and ~~(01 $\bar{1}$)_{cub}~~ planes, the traces being aligned along $\langle 1\bar{1}1 \rangle_{\text{cub}}$ and $\langle \bar{1}11 \rangle_{\text{cub}}$ ^[11]. They are very characteristic, forming a 'V' shape (Fig. 1), the obtuse angle being $2 * 54.7^\circ (= 109.4^\circ)$ and the acute one $2 * 35.3^\circ$

/(10 $\bar{1}$)_{cub}

(= 70.6°). Here, we neglect the rhombohedral distortion. The obtuse and acute bisectrix give the $\langle 001 \rangle_{\text{cub}}$ and $\langle \bar{1}10 \rangle_{\text{cub}}$ directions, respectively. On a very thin $(110)_{\text{cub}}$ cut, traces of $(\bar{1}\bar{1}0)_{\text{cub}}$, $(100)_{\text{cub}}$ and $(010)_{\text{cub}}$ domain walls are of course parallel and traces of $(001)_{\text{cub}}$ walls perpendicular to a $\langle 001 \rangle_{\text{cub}}$ direction, respectively.

As mentioned above, in order to measure the principal birefringence dn , thin $(110)_{\text{cub}}$ crystal platelets were not available, having \vec{P}_s , the spontaneous polarization, and hence the optical axis (OA// \vec{P}_s), in the plane of the platelet. The optical axis of the used crystal was inclined at about 35.3° to the platelet normal \vec{N} . Under a polarizing microscope with crossed polarizer and analyzer, using orthoscopy (parallel light illumination), inclined edges of all BiFeO₃ crystals appeared black, because of the high \bar{n} value (total reflection). Therefore, it was not possible to count the number of interference fringes along an edge of the crystal, even using an immersion oil, in order to deduce an approximate value of the optical retardation. Conoscopy, on the $(110)_{\text{cub}}$ plate ($t = 11 \mu\text{m}$), with crossed polars, using immersion oil ($n_e = 1.518$), high numerical aperture ($NA = 1.40$ oil) front lens on the condenser and high numerical aperture objective (100 \times /1.30 oil) was an invaluable help to deduce the interference order at room temperature, even though the melatope, the trace of the optical axis, was outside the field of view. By observing the motion of the isogyre when rotating the microscope stage, thus rotating the crystal, it was deduced that the first to the fifth isochromes for green light (551 nm) and the first to the fourth isochromes for red light (643 nm) were inside the conoscopy field of view (Fig. 2).

Graphical simulation confirms this deduction, by plotting the refractive index ε' vs. θ , where θ is the angle between the optical axis OA (// \vec{P}_s) and an oblique ray of light inside the crystal, in the plane formed by \vec{P}_s and \vec{N} (the normal to the cut). A first curve is traced (ε' vs. θ), using the equation of the indicatrix (an oblate ellipsoid of revolution)

$$\varepsilon' * (\cos^2\theta/\omega^2 + \sin^2\theta/\varepsilon^2) = 1 \quad (1a)$$

and a second set of curves is traced (ε' vs. θ), by computing the optical retardation of an inclined ray of light, inside the crystal, which must be equal to an integer times the wavelength

$$\Gamma(\theta_k) = t * (\omega - \varepsilon')/\cos((\pm)\alpha + (\mp)\theta_k) = k * \lambda, \text{ with } \alpha = 35.3^\circ, k = 1, 2, \dots \quad (1b)$$

The intersections of this latter set of curves with the former one give, θ_k and thus the order k of the isochrome curves. Because of the high mean

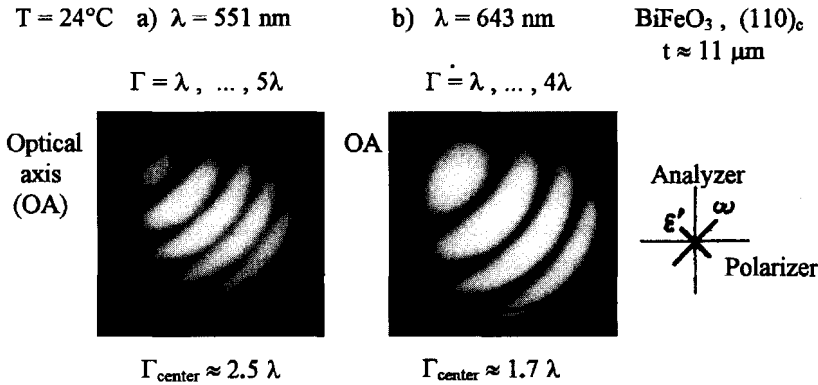


FIGURE 2 Room temperature conoscopy of a BiFeO₃ ferroelastic single domain crystal ($t = 11 \mu\text{m}$), a (110)_{cub} cut, with \vec{P}_s and the optical axis at 35.3° away from the normal to the cut. Condensor's numerical aperture: 1.4 oil, objective: 100 x/1.3 oil. a) $\lambda = 551 \text{ nm}$, b) $\lambda = 643 \text{ nm}$. Interference orders have been identified (see text). The center of the field of view gives the plate retardation.

refractive index and the high birefringence values of this crystal, this simulation is an approximation. Nevertheless, the correct interference orders ~~and~~ obtained.

Approximate platelet retradations Γ' are obtained by evaluations of the relations at the center of the conoscopic figures ($\Gamma'(551\text{nm}) \approx 2.5 * \lambda \approx 2.5 * 551 \text{ nm} \approx 1378 \text{ nm}$ and $\Gamma'(643 \text{ nm}) \approx 1.7 * \lambda \approx 1.7 * 643 \approx 1093 \text{ nm}$) and approximate platelet birefringences dn' by dividing the retradations by t , the thickness of the plate (t and Γ' in nm): $dn'(551 \text{ nm}) = \Gamma'/t \approx 0.125$ and $dn'(643 \text{ nm}) \approx 0.099$.

are
retardations

To a first approximation one obtains from the equation of the optical indicatrix of a uniaxial crystal and in the case of small birefringence:

$$dn' \approx dn * \sin^2\theta \tag{2}$$

where $\theta = \alpha/35.3^\circ$ is the angle between the optical axis (OA // \vec{P}_s) and the normal (\vec{N}) to the (110)_{cub} platelet. Thus:

$\lambda \approx$

$$dn \approx 3 * dn' \tag{2'}$$

Then the principal birefringence of this BiFeO₃ crystal is given by: $dn(643 \text{ nm}) \approx 3 * 0.1 \approx 0.3$, which is consistent with the result obtained from another method given below.

At this point, one has to note that a value twice as large as this one – which is already very large – was measured with a (10 order) tilting

compensator, due to erroneous determination of the compensation order. For, with white light, by observing a birefringent crystal oriented at 45° between crossed polars, the standard Newton interference colors, as can be seen on a Michel-Levy chart, could be dramatically modified because of absorption, dichroism, anomalous dispersion and combination of these phenomena. Thus the "right" compensation interference line which should appear black could appear colored! Due to this fact, an error of one or some interference order(s) could easily be made. Textbooks on crystal optics, mineralogy and operating manuals of polarized light microscope components usually do not mention this problem, although crystals with e.g., transition elements and thus absorption and dichroism, are very common.

Beugnies^[12] suggested a method in order to find the order of interference, for crystals which are transparent in the infrared (IR) or near-IR (NIR) only. It consists to measure, photoelectronically, the retardations of a number of interference orders at two wavelengths, λ_1 , λ_2 with $\lambda_1 \approx \lambda_2$. It should be possible to find a retardation value for which:

$$\Gamma(q) \approx \Gamma_2(\lambda_2) \approx \Gamma(\bar{\lambda}) \quad (3).$$

Weak birefringence and "normal" dispersion are implicitly admitted, as it is sometimes the case in the NIR. However, as will be shown, this method has to be applied cautiously in the case of large retardation. A practical method, is to plot the retardation at two different wavelengths vs. "subtraction" and "addition" orders (q). Numbering the orders (q) may be done arbitrarily. Straight lines are obtained which should cross close to an integer number. This gives the retardation at compensation (as well as the "subtraction" orientation of the crystal) but the crystal thickness and (true) birefringence dispersion near $\lambda_1 \approx \lambda_2$ must fulfil the following inequality^[13]:

$$t * |dn(\lambda_1) - dn(\lambda_2)| < |\lambda_1 - \lambda_2|/2 \quad (4)$$

Figure 3 shows the application of this method for this BiFeO₃ crystal ((110)_{sub}cut) which has an inclined OA out of the crystal plane ($\alpha = \angle(\vec{N}, \vec{P}_s) \approx 35.3^\circ$). A microphotometer was inserted between the ocular of a polarizing microscope and a photomultiplier tube (PMT) in order to select a small single domain of the crystal to be measured. While performing the experiments, a number of monochromatic interference filters ($4 \text{ nm} < \text{HW} < 12 \text{ nm}$) were inserted into a slot of the microphotometer. On the microscope base, a photoelastic modulator (PEM) was fixed at 45° with respect to a linear polarizer and just above it. The polarization state of

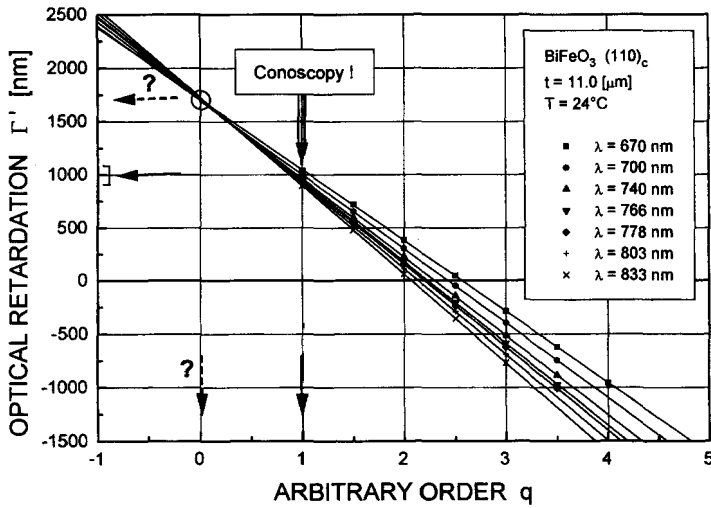


FIGURE 3 Same crystal as in Figure 2. Optical retardation vs. (arbitrary) retardation order, measured with a Babinet-Soleil compensator and a photoelastic modulator to increase the sensitivity. About the method, see text. Retardation values for integer and half-integer q values can be obtained with a 'lock-in' amplifier. Because of large birefringence, the intersection of two successive straight lines gives a retardation apparently one order larger.

the light is then modulated at a fixed frequency $f = 50$ kHz. High optical retardation sensitivity is obtained with a 'lock-in' amplifier (at f) and a Babinet-Soleil compensator^[14a]. From Figure 3, it can be seen that for some wavelengths in the NIR, from $\lambda = 670$ nm to 833 nm, the lines cross each other close to the relative order $q = 0$ but the retardation values obtained by conoscopy were consistent with $q = 1$! Finally, Figure 4 shows the birefringence dispersion curve $dn'(\lambda)$ for this (110)_{cub} cut, using the retardation order as deduced by conoscopy. The fact that Eq. (4) is not fulfilled for any two successive filters confirms that $q = 0$ is not the right relative order, thus Beugnie's^[12] method is not applicable in the present case.

retardation
~
retardation
~

A similar graph as the one in Figure 3 was simulated by taking the birefringence values of a calcite crystal ($dn \approx 0.17$, at $\lambda = 550$ nm) having the same thickness ($t = 11 \mu\text{m}$) as the used BiFeO₃ crystal, confirming once more the fact that in the case of crystals with large optical retardation, this method of tracing straight lines ($\Gamma(q) \approx a_{\lambda 1}q + b_{\lambda 1} \approx a_{\lambda 2}q + b_{\lambda 2}$) for finding the retardation order q should be used cautiously.

To compute the principal birefringence of a (negative) uniaxial crystal, from an inclined cut, one has to compute $dn = \omega - \epsilon$ knowing $dn' = \omega - \epsilon'$. Due to the large birefringence, the approximation $dn \approx 3 * dn'$ (when

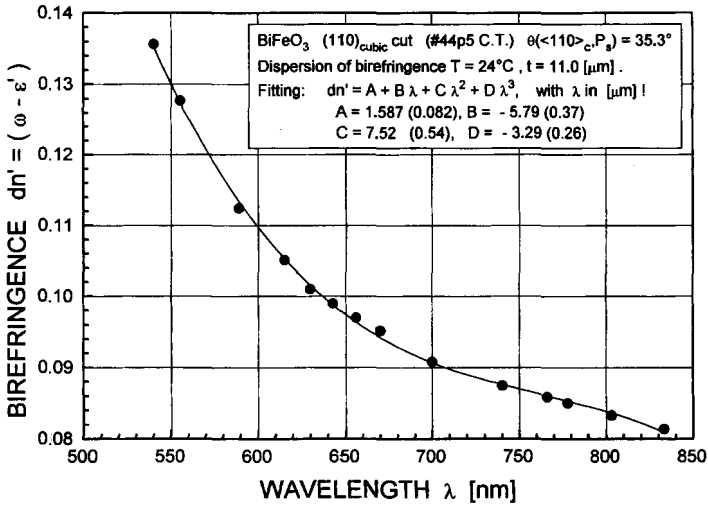


FIGURE 4 Same crystal as in Figure 2. Birefringence dispersion $dn' = \omega - \varepsilon'$, $T = 24^\circ\text{C}$. $\lambda(\lambda)$

$\alpha \approx 35.3^\circ$, Eq. (2')) is no more valid and hence the refractive indices ω , ε and ε' must be measured or computed independently. As already mentioned for BiFeO_3 , only a mean refractive index \bar{n} has been obtained by the Gladstone-Dale relationship. We have the following system of 3 equations with 3 unknowns (ω , ε , ε'):

$$2\omega + \varepsilon \approx 3\bar{n}, \quad \omega - \varepsilon' = dn' \quad \text{and} \quad (\cos^2\alpha/\omega^2) + (\sin^2\alpha/\varepsilon^2) = 1/\varepsilon'^2 \quad (5a - 5c)$$

with $\bar{n} \approx 2.62$, $dn'(\lambda = 550 \text{ nm}) \approx 0.130$ and $\alpha \approx 35.3^\circ$. We assume the Gladstone-Dale relationship to be valid for $\lambda = 550 \text{ nm}$, which is rather arbitrary, and use the measured value of dn' at this same wavelength. An easy way to solve this system is with a software for symbolic computation (e.g., *Maple V*), with an execution time to solve of about 1 s, needing only one or two instruction line(s).

The principal birefringence of a BiFeO_3 crystal at room temperature and at $\lambda = 550 \text{ nm}$ is then $dn = \omega - \varepsilon \approx 2.731 - 2.389 \approx 0.34$, compared to $dn \approx 3 \cdot 0.13 \approx 0.39$, using Eq. (2'). To obtain a first estimation of the dispersion of $dn(\lambda)$, we use Eq. (2') again and Figure 4. A variation of $\Delta dn' \approx 0.01$, corresponds to $\Delta dn \approx 3 \cdot \Delta dn' \approx 3 \cdot 0.01 \approx 0.03$. Concerning the accuracy one has to remember that the thickness of this crystal is known to about 10%. The accuracy on \bar{n} , computed with the Gladstone-Dale relationship, is unknown!

Another problem was to try to detect the magnetic phase transition \wedge BiFeO₃ optically, at T_N . Because the edge of the charge transfer absorption band ($\text{Fe}^{3+} \leftrightarrow \text{Fe}^{2+}$) shifts to longer wavelength^[3], i.e., to the red, by increasing the temperature, the measurements were done in the near IR, at $\lambda = 740$ nm. A new method^[14] has been set up to measure, linearly vs. temperature, the linear birefringence, without any compensator or by using it as a fixed wave plate, to translate the crystal's retardation. The linearly polarized light is again modulated by a PEM. The DC and one of the AC signal components from the PMT are separated and measured with a DC voltmeter and a lock-in amplifier, respectively. Under a particular adjustment of the PEM, one obtains a linear function of the optical retardation variation over a large range ($\Delta \Gamma = \lambda/2$). Figure 5 shows $dn'(T)$, i.e., $\omega - \varepsilon'$ around T_N , taking the derivative of this curve, $T_N \approx 380^\circ\text{C}$ ($\pm 3^\circ\text{C}$) or $T_N \approx 653$ K (± 3 K). The natural logarithm of the difference between the extrapolated (straight line) birefringence from above T_N and dn' below T_N has been plotted vs. the natural logarithm of the reduced temperature^[14b]. From the slope, an exponent of $2\beta = 0.85$ has been obtained ($\Delta(dn') = B \cdot ((T_N - T)/T_N)^{2\beta}$, $0.93 < T/T_N < 0.994$) even though the cut is not a principal one and the true base line is not known accurately! From Mössbauer experiments a value of $T_N = 655$ K was found, close to our

\wedge of

/ [13]

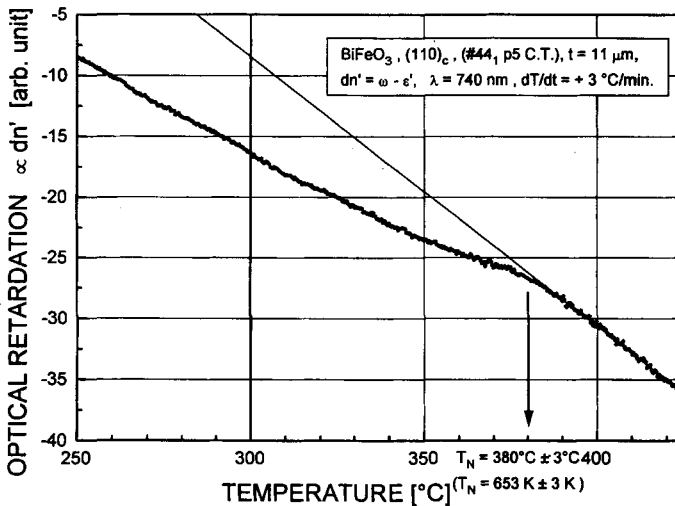


FIGURE 5 Same crystal as in Figure 2. First optical determination of $T_N \approx 653$ K (380°C) from the birefringence: $dn'(T)$, $\lambda = 740$ nm, with the help of a photoelastic modulator, a DC voltmeter and a 'lock-in' amplifier.

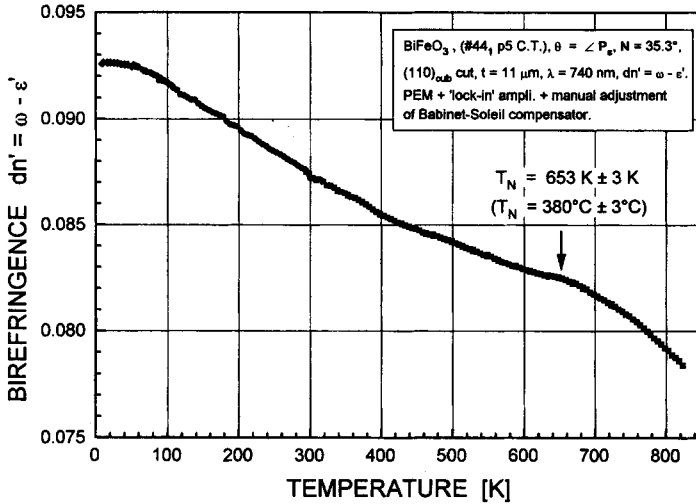


FIGURE 6 Same crystal as in Figure 2. Birefringence of BiFeO_3 , $8 \text{ K} < T < 820 \text{ K}$: $dn'(T) = \omega - \epsilon'$, $\lambda = 740 \text{ nm}$.

determination, and a critical exponent $\beta = 0.37$ ($0.90 < T/T_N < 0.99$) computed from the temperature dependence of the hyperfine field^[15].

The birefringence $dn'(T)$ of this $(110)_{\text{cub}}$ cut is given in Figure 6, from 8 K to 820 K (547°C), using the same method and with the calibration at room temperature as given in Figure 4. No magnetic field was applied.

Another test by conoscopy, with monochromatic light, on a $(111)_{\text{cub}}$ cut BiFeO_3 crystal ($t = 29 \mu\text{m}$), perpendicular to OA and \vec{P}_s , showed that the number of isochromes in the field of view (objective $100\times/1.3$ oil and front lens condenser 1.4 oil) was consistent with the principal birefringence value deduced from the oblique cut.

CONCLUSION

The birefringence dispersion curve ($T = 24^\circ\text{C}$) of an oblique $(110)_{\text{cub}}$ BiFeO_3 crystal cut ($\angle(\vec{N}, \vec{P}_s) \approx 35.3^\circ$) was measured, showing "normal" dispersion character and an estimation of the principal birefringence gives $dn(\lambda = 550 \text{ nm}, T = 24^\circ\text{C}) \approx 0.34$ which is very large but not as large (0.6) as mentioned in our former publication.

The birefringence vs. temperature in the near IR, of this same $(110)_{\text{cub}}$ cut, has been measured with the help of a photoelastic modulator and 'lock-in' analyzer. The Néel temperature is $T_N = 653 (\pm 5) \text{ K}$ or $380 (\pm 5)^\circ\text{C}$.

$\lambda \approx$
 $\lambda [3]$

~~XXXX~~

Owing to the large birefringence of BiFeO₃, probably only a very thin, less than 10 μm, (110)_{cub} principal cut could serve to measure its exact birefringence value. Correction ~~for~~ reflectivity should also be taken into account. / for

Acknowledgements

The crystals used in this work were synthesized and prepared by Dr. C. Tabares-Muñoz. The authors would like to thank R. Boutellier for technical help and the Swiss National Science Foundation for support.

References

- [1] Sosnowska, I., Peterlin-Neumaier, T. and Steichele, E. (1982). *J. Phys. C: Solid State Phys.*, **15**, 4835.
- [2] Sosnowska, I., Przenioslo, R., Fischer, P. and Murashov, V. A. (1994). *Acta Phys. Pol.*, **8G**, 629.
- [3] Tabares-Muñoz, C., Rivera, J.-P. and Schmid, H. (1984). *Ferroelectrics*, **55**, 235.
- [4] Preset paper.
- [5] Kubel, F. and Schmid, H. (1990). *Acta Cryst.*, **B46**, 698.
- [6] Tabares-Muñoz, C., Rivera, J.-P., Bezings, A., Monnier, A. and Schmid, H. (1985). *Jpn. J. Appl. Phys.*, **24**, Suppl. 24-2, 1051.
- [7] Popov, F. Yu., Vorobiev, G. P., Zvezdin, A. K., Kadomtseva, A. M. and Kazei, Z. A. (1993). *Bull. Rus. Ac Sc. Phys.*, **57**, 1109.
- [8] Popov, F. Yu., Kadomtseva, A. M., Vorob'ev, G. P. and Zvezdin, A. K. (1994). *Ferroelectrics*, **162**, 135.
- [9] Tabares-Muñoz, C., Ph. D. Thesis (1986). No. 2191, University of Geneva.
- [10] Mandarino, J. A. (1976). *Can. Mineral.*, **14**, 498.
- [11] The walls orientation are analogous to the case of rhombohedral boracites: H. Schmid, (1970). *Phys. Stat. Sol.*, **87**, 209.
- [12] Beugnies, A. (1969). "Microscopie des milieux cristallins", Presses Académiques Européennes, Bruxelles and Dunod, Paris, Ch. VIII, 117-118.
- [13] Rivera, J.-P. to appear.
- [14] Ferré, J. and Gehring, G. A. (1984). *Rep. Prog. Phys.*, **47**, 513, a) Ch. 2, b) Ch. 5 § 3.1.2. (i).
- [15] Blaauw, C. and van der Woude, F. (1973). *J. Phys. C: Solid State Phys.*, **6**, 1422.